

## Griffith Cracks at the Nanoscale

**Sheldon M. Wiederhorn**<sup>\*,†</sup>

*National Institute of Standards and Technology, Gaithersburg, Maryland 20899*

**Theo Fett**

*Karlsruhe Institute of Technology, Institute of Applied Materials, 76131 Karlsruhe, Germany*

**Jean-Pierre Guin**

*LARMAUR, ERL 6274 (CNRS University of Rennes 1), 35042 Rennes, France*

**Matteo Ciccotti**

*Laboratoire PPMD/SIMM, UMR 7615 (CNRS, UPMC, ESPCI Paristech) 10 rue Vauquelin, 75005 Paris, France*

---

When Griffith presented his famous theory of crack stability in elastic materials in the early twentieth century, he was unable to provide much detail on the structure of cracks at the nanometer level of resolution. Now, almost 100 years later, techniques such as transmission electron microscopy, atomic force microscope, nuclear reaction analysis, and nuclear reflection are available to achieve this level of resolution. Here, we review the kind of data obtained using these techniques and the implications of the data vis-à-vis cracks in silicate glasses. Measurements by atomic force microscopy provide information on the size of the nonlinear zone at crack tips in glass, on environmental conditions at crack tips, and on the possibility of cavity formation as a mechanism of crack growth. Examination by nuclear reaction analysis and neutron reflection of fresh fracture surfaces formed in water has yielded information on water penetration through the glass surrounding the crack tip, to a resolution of 3–5 nm. Improvement of measurement techniques in the coming years should enable us to study crack tips in glasses to even higher levels of resolution and to answer more detailed questions concerning the level of stress and the size of the nonlinear zone at the crack tip.

---

### Introduction

In his seminal paper, “The Phenomena of Rupture and Flow in Solids,” Griffith<sup>1</sup> demonstrated that the

strength of a soda lime silicate glass was inversely proportional to the square root of the length of cracks in the glass surface. He generalized this finding to conclude that planar defects, such as cracks, were the primary factors controlling the strength of structural materials. This dependence of strength on crack length eventually was transformed into the science of Fracture

---

<sup>\*</sup>Member, The American Ceramic Society.

<sup>†</sup>sheldon.wiederhorn@nist.gov

Mechanics,<sup>2</sup> which is currently part of the accepted methodology used to assure the reliability of structural materials. Although the Griffith theory gave an enormous boost to engineering practice and to our understanding of the failure of structural materials, the theory gave little insight into the molecular fundamentals of the fracture process. These fundamentals are important for it is at this level of understanding that the mechanism of fatigue and of subcritical crack growth are determined for structural materials. Factors of importance include the shape of the crack tip, whether it is atomically sharp or has been blunted by plastic deformation of the material surrounding the crack tip or by chemical corrosion caused by the surrounding environment. Since the time of Griffith, experimental techniques, such as transmission electron microscopy and atomic force microscopy, have been developed to reveal details of the crack tip structure almost to the molecular level. These details provide a substantial database that can be used to understand and to improve the behavior of structural materials under applied loads.

In ceramic materials, the molecular structure of the crack tip has been a subject of investigation for over 50 years. Early studies on glasses revealed that nonrecoverable plastic impressions were formed under scratches and indentations caused by sharp diamond points;<sup>3</sup> similar observations were made on crystalline materials such as aluminum oxide and silicon carbide.<sup>4</sup> With this evidence, it was natural to suggest that plastic deformation could also occur at crack tips in these materials. Lawn *et al.*<sup>5</sup> dismissed this possibility and suggested that plastic deformation in the vicinity of indentations cannot be taken as evidence of plastic deformation at crack tips, because plastic deformation at indentations occurs within the constraints of a triaxial compressive stress field, which suppresses crack formation, whereas at crack tips, the reverse is true.<sup>5,6</sup> The question of crack tip deformation was quantified by Kelly *et al.*<sup>7</sup> who argued that crack tip plasticity occurs if the cohesive strength of the material in shear is exceeded before the tensile strength is reached. A similar argument was made earlier by Griffith.<sup>1</sup> Rice and Thomson<sup>8</sup> supported this view by developing conditions for dislocation generation at crack tips in crystals. These authors predicted that metallic crystals would have dislocations generated from their crack tips, whereas crack tips of covalent inorganic materials would be free of dislocations, especially at low tempera-

tures. In support of these predictions, transmission electron microscopy studies on SiC, Al<sub>2</sub>O<sub>3</sub>, Si, Ge, and SiAlON<sup>4,5,9-12</sup> found no dislocations at crack tips at room temperature. At higher temperatures, however, dislocations were observed in Si, 500°C<sup>4,5</sup> and Al<sub>2</sub>O<sub>3</sub>, 600°C.<sup>9</sup>

Glasses, which are amorphous and cannot diffract electrons, present a special challenge to the evaluation of crack tip structures. Only absorption contrast is useful for distinguishing features at crack tips by TEM, and only one study has been made using TEM to characterize cracks in silica glass.<sup>13</sup> The authors found a crack tip with the expected parabolic dependence of crack width on crack length, which is characteristic of a linear-elastic material. Also, the estimate of the crack tip radius, 1.5 nm, was that expected for a linear-elastic crack with the shape of an ellipse. However, this result is controversial, because a measurement of the far field crack opening displacement yielded an applied stress intensity factor for the crack of 2.7 MPa m<sup>1/2</sup>, which is three to four times the measured value of the critical stress intensity factor,  $K_{Ic} = 0.8$  MPa m<sup>1/2</sup>.<sup>14</sup> Thus, the shape of the crack observed by Bondo *et al.*<sup>13</sup> may not have been determined by purely linear-elastic considerations alone.

Advances in our understanding of crack tip structure of glass have been obtained more recently, not by transmission electron microscopy, but by atomic force microscopy (AFM). The method works by scanning the surface with a very sharp probe (see reference 15 for a review of the technique) and measuring the position of the probe, both in the surface, the  $x$ - $y$  plane, and in the direction above the scanning plane, the  $z$  direction. Commercial instruments have a measurement capability of approximately 0.05 nm in the  $z$  direction and approximately 1–10 nm in the  $x$ - $y$  plane, depending on the sharpness of the probe and the mode of scan (contact mode or intermittent contact mode). The  $z$  resolution gives near atomic resolution for the AFM. For details on how the AFM may be used to study cracks in glass, reference (16) is recommended.

This article discusses recent experimental measurements and theoretical calculations relevant to the structure of crack tips in glass. The article is a follow-up to an earlier paper on this subject.<sup>16</sup> Topics discussed include surface displacements at crack tips, water diffusion into the tips of cracks during fracture, the size of the nonlinear zones at crack tips, and environmental conditions at crack tips. Information on crack tips can be obtained both by direct examination of the crack tip

*in situ* and by examining the fracture surface after completion of the fracture process.

### Use of the AFM to Study Crack Tips in Glass

In the *in situ* technique, the crack tip is scanned, at a point where the tip emerges at a “free surface” of the glass specimen.<sup>17</sup> The stresses associated with the crack tip displace and warp the free surfaces of the specimen, Fig. 1. These nm magnitude displacements can be compared with displacements calculated from an elastic solution of the crack geometry. Any discrepancy between the measured and calculated displacements is assumed to be due to crack tip plasticity or some other nonlinear effect at the crack tip. From these calculations, it is possible to ascertain the size of a plastic zone at the crack tip. It is also possible to use the AFM in the scanning mode to measure the magnitude of capillary forces when a condensate fills the tip of a crack or localized stresses around the crack tip resulting from ion exchange<sup>18</sup> or water penetration into glass.<sup>19,20</sup>

The second technique of characterizing a crack is to scan the fracture surface after the specimen has been broken in two. This is a standard technique used in field of fractography to understand physical processes occurring at crack tips. Use of the AFM for this pur-

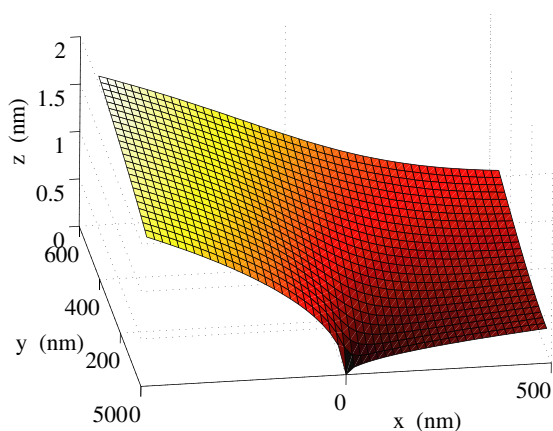


Fig. 1. Schematic of the  $z$  displacement (the surface depression) around the point of crack emergence of a crack tip through the free surface perpendicular to the scanning direction.<sup>24</sup> In this depiction, the  $z$  displacement at 500 nm from the crack tip is about 1.5 nm. As the displacements are symmetric across a mirror plane containing the  $x$  axis, only one-half of the surface surrounding the crack tip is shown.

pose permits one to investigate the surface at high magnification and in three dimensions. The technique can be used to study corrosion at crack tips in glass, ion exchange at the crack tip ( $\text{Li}^+$ ,  $\text{Na}^+$ , or  $\text{K}^+$  for  $\text{H}_3\text{O}^+$  in the crack tip condensate), and water penetration into silica glass and the consequent swelling of that glass.

### Measurement of Nanoscale Crack Tip Displacement Fields

Depending on the nonlinear process occurring at the crack tip, the crack tip opening displacement can range from one nm for a completely elastic crack to several nm for a crack tip that has undergone significant plastic deformation. Outside of the nonlinear zone, the displacements should be entirely elastic. The methodology for characterizing the size of a nonlinear zone surrounding a crack tip in glass by measuring the surface displacements and comparing them with an elastic solution was first suggested and tried by Célarie *et al.*<sup>17</sup> on a crack in a double cleavage drilled compression specimen (DCDC).<sup>21–23</sup> Unfortunately, there were two problems with their experiment. First, a full three-dimensional solution of the equations of elasticity was needed for an accurate prediction of the surface displacements; Célarie *et al.* used a two dimensional approximation, which leads to serious errors in predicting displacements at the crack tip.<sup>††</sup> Second, Célarie *et al.* neglected taking into account the roughness of the free surface, which can be as large as the displacements being measured on the AFM images around the crack tip.

The first experiment to handle both the surface roughness and elastic displacements correctly was that by Han *et al.*<sup>24</sup> These authors measured both the out-of-plane and in plane displacements of the free surface surrounding an emerging crack in a DCDC specimen of silica glass. They used a complete solution of the elastic displacements surrounding the point of emergence of a crack in the specimen<sup>25</sup> to calculate the theoretical displacements surrounding the crack tip, Fig. 1. Han *et al.*<sup>24</sup> eliminated the effect of surface roughness using an extension of the Digital Image Correlation (DIC) technique.<sup>26</sup> The technique is applied to two

<sup>††</sup>The solution presented by Célarie *et al.*<sup>17</sup> assumed that the out of plane displacement of the free surface,  $u_z$ , goes as  $-r^{-1/2}$  as  $r$  approaches zero, where  $r$  is the distance from the crack tip. Therefore,  $u_z$  goes to negative infinity as  $r$  approaches zero, which is a breach in the assumptions of continuity.

AFM images, the reference image and the deformed image, taken on the same surface at two different times, the crack length increasing during the time interval. The  $z$  displacements of the reference image (Fig. 2a) are subtracted from the  $z$  displacements of the deformed image (Fig. 2b), which removes the roughness of the surface from the image. The difference between the two experimental images (not shown) is compared with the difference calculated from a full, three-dimensional solution of the elastic crack tip displacement field (Fig. 2c). The calculated image (Fig. 2c) can then be subtracted from the experimental image (the difference between Figs. 2b and 2a), which yields the residual map, Fig. 2d. The residuals in Fig. 2d are all less than approximately  $\pm 0.2$  nm, which is the order of atomic distances in the glass being studied, suggesting that at distances  $>10$  nm from the crack tip, surface displacements surrounding the crack tip are

elastic to within the experimental scatter given by the residuals of the measurement.

The crack tip displacements can also be used to estimate a value of the crack tip stress intensity factor. The value obtained,  $K_I = 0.39 \pm 0.04 \text{ MPa m}^{1/2}$ , agrees well with the value measured macroscopically using DCDC specimens,  $K_I = 0.39 \pm 0.02 \text{ MPa m}^{1/2}$ . The technique of Digital Image Correlation also allows for a more accurate estimation of the crack opening profile than direct analysis of the crack lip shape as performed in reference (5).

The experiment carried out by Han *et al.*<sup>24</sup> is significant because it sets an upper limit to the possible size of the nonlinear zone around a crack tip in glass. The size of the nonlinear zone in silica glass has to be smaller than 10 nm. This result casts doubt on the observation of Prades *et al.*<sup>27</sup> that cavities of the order of 125 nm are formed at the tips of propagating cracks in silica, see

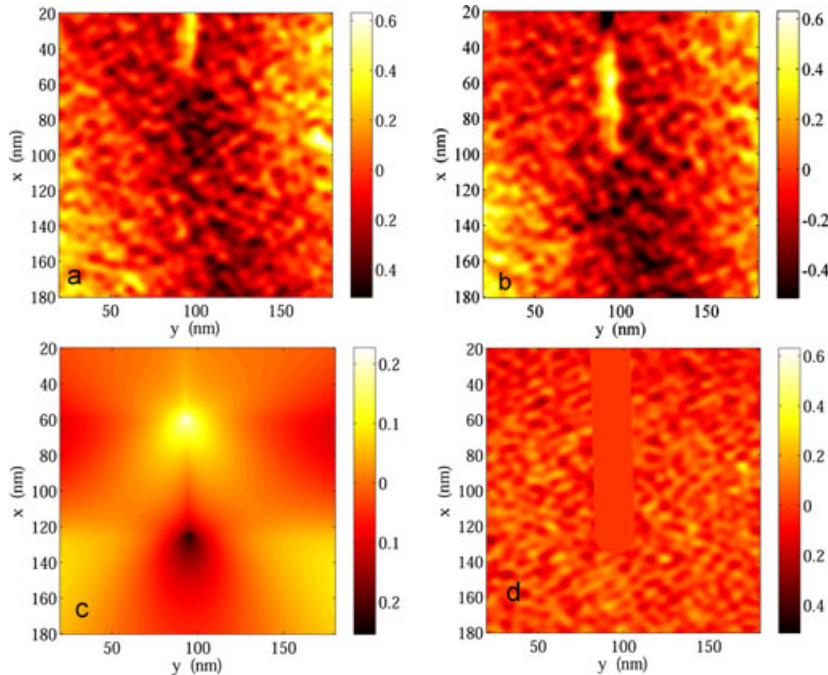


Fig. 2. Example of digital image correlation (DIC) analysis of the out-of-plane displacement field on a couple of  $200 \mu\text{m}$  size topographic images at two stages of crack propagation.<sup>7</sup> (a) Reference image. (b) Deformed Image. (c) Image difference (theoretical) calculated from reference (24). (d) Residual map. The mask around the image is 10 nm from the crack surface; this is the estimated uncertainty of the lateral measurement distance in the plane of measurement. The bright yellow color at the crack tip, (a and b) is a false high caused by condensate in the crack tip. This region is shielded by the mask and is not included in the calculation. The dark spot in (c) represents the crack tip from (b); the bright spot in (c) represents the crack tip in (a) (subtraction reverses the displacement direction, hence the color difference). The color bars to the right of each figure indicate an absolute measurement of height from the zero point indicated by the orange color.

discussion below. This technique has yet to be applied to crystalline materials such as silicon or sapphire.

$$\sigma_{yy} = \frac{2K}{\sqrt{\pi\rho}} \quad (2)$$

### On the Size of the Plastic Zone

Given that the nonlinear zone in silica glass has to be less than 10 nm, one might ask the following question: how much smaller can the non-linear zone be and what will the resolution have to be for it to be detected? It is safe to say that its size will depend on detailed structure of the glass at the crack tip and any processes such as plastic deformation that occur at crack tips in silica glass. Estimates of the expected size of the nonlinear zone can be made from continuum calculations, such as the Dugdale–Barenblatt model of a plastic zone at a crack tip in a continuum.<sup>28,29</sup> The size of the zone is given by Eq. 1:

$$R = (\pi/8)(K_{IC}/\sigma_y)^2 \quad (1)$$

where  $K_{IC}$  is the critical stress intensity factor, and  $\sigma_y$  is the yield strength of the glass. The yield stress for silica glass has to be at least equal to the maximum measured tensile strength of the glass 12.6 GPa.<sup>30</sup> Substituting  $0.8 \text{ MPa m}^{1/2}$  for  $K_{IC}$ <sup>14</sup> and 12.6 GPa for  $\sigma_y$ , the estimated plastic zone size equals 1.6 nm, which is several times the size of the silica tetrahedra rings in silica glass, that is,  $\approx 0.5 \text{ nm}$ . This observation has been noted earlier by other investigators, see for example reference (31).

The minimum size of the nonlinear zone can also be estimated from an elastic model with molecular structure at the crack tip. Linear-elastic fracture mechanics deal with cracks in a material that is continuous up to the sharp crack tip. This requirement is of course not fulfilled in real materials, which must become nonlinear as atomic dimensions at the crack tip are approached. In silica, the  $\text{SiO}_2$ -structure forms rings of  $\text{SiO}_2$ -molecules with different numbers of molecules included in each ring. The larger gaps between the molecules can be considered as nanopores. Considering these nanopores as perturbations in the sense of Saint Venant, we have to expect validity of continuum mechanics for volume elements of at least 3 times the perturbation size, *that is*,  $\approx 1.5 \text{ nm}$ .

A crack with such a pore at its end, then behaves as a fictitious slender notch with finite notch-root radius,  $\rho$ . The stresses ahead of the notch root were derived by Creager and Paris.<sup>32</sup> The normal stress directly ahead of the root is given as

The stress,  $\sigma_{yy}$ , will be higher than the experimental strengths measured on high-strength optical fibers, due to the unavoidable presence of surface defects in these fibers.<sup>33</sup> Having in mind the extremely small effective surfaces and volumes ahead of a crack tip, the theoretical limit strength is used in Eq. 2. Failure of glass occurs when the stress reaches the theoretical strength,  $\sigma_{\text{theor}} \cong E/\pi \cong 23 \text{ GPa}$ . With  $K_I = 0.8 \text{ MPa m}^{1/2}$ , this yields an *effective notch radius*  $\rho_{\text{eff}} = 1.54 \text{ nm}$ .

From the above considerations, we conclude that to detect the nonlinear zone in silica glass, the  $x$ - $y$  resolution of the AFM probe will have to be approximately 1–2 nm, which means using a sharper probe, taking care that it is not blunted while scanning the surface. Probably, a noncontact probe will have to be used for this purpose. Whether this level of accuracy and repeatability can be achieved with current available techniques remains to be seen.

### Cavity Formation at Crack Tips in Silica Glass

In a discussion of the possibility of crack growth in glass by the nucleation, growth and coalescence of cavities at crack tips, Célarie *et al.*<sup>17</sup> and Prades *et al.*<sup>27</sup> suggested that they had experimental evidence that cavitation caused crack growth in glass. By observing the tips of growing cracks in an aluminosilicate glass<sup>17</sup> and in a silica glass,<sup>27</sup> these authors observed a depression leading the tip of the crack and saw what looked like cavities forming in front of the crack. They concluded that the experimental evidence supported a mechanism for crack growth similar to that shown in Fig. 3.<sup>34</sup> The size of the cavities reported were 20 nm long by 5 nm deep for an aluminosilicate glass<sup>17</sup> and 125 nm long by 25 nm deep for a silica glass.<sup>27</sup>

Later, Guin and Wiederhorn<sup>35</sup> argued that if cavities formed at the tips of cracks in glass, some trace of them should be visible on the fracture surface. These authors examined surfaces of soda lime silicate glass and silica glass using atomic force microscopy to obtain topographs of the matching fracture surfaces. In comparing the two surfaces, they expected to find voids where the crack intersected the cavities, *that is*, the surfaces would not match. In contrast to their expectations, profiles from the opposing fracture surfaces matched very well, as shown

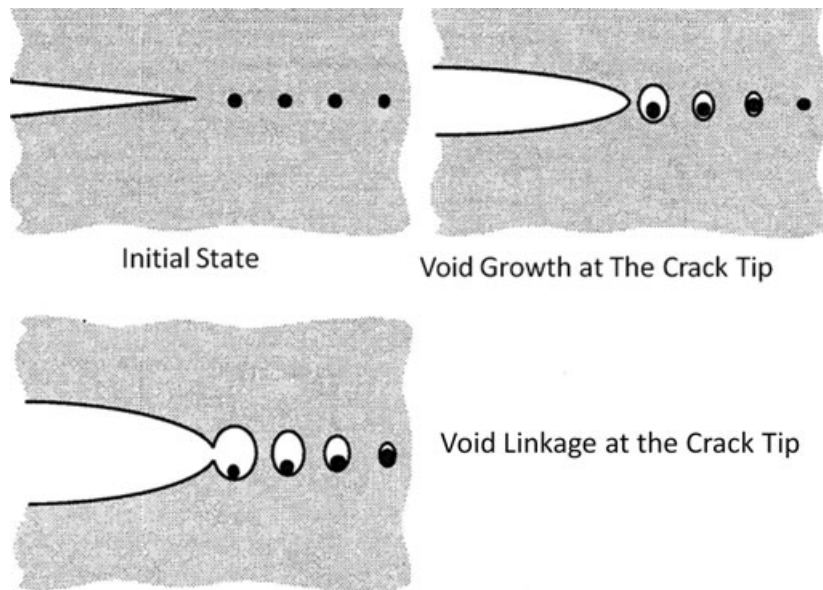


Fig. 3. Mechanism for ductile crack growth. Plasticity develops around defects, or foreign particles in the solids, followed by the generation and growth of voids. The rate of void linkage accounts for the rate of crack growth. Discussed in reference (34).

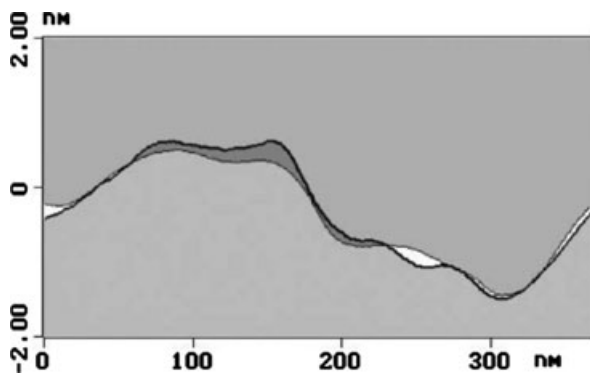


Fig. 4. Results of sectioning a crack along the same cut in both fracture surfaces: silica glass. The crack propagated from left to right at a velocity of about  $3 \times 10^{-7}$  m/s.<sup>35</sup>

for silica in Fig. 4. A fuller discussion of this subject is given in reference (36), in which the authors attribute the observations in references (17,27) not to cavities, but to the roughness of the specimen surface and natural elastic displacements that occur when a sharp crack intersects a surface.

Molecular Dynamics (MD) simulations<sup>37</sup> have also suggested a cavity coalescence mechanism of crack growth in silica, in which nanometer size cavities are generated at the tip of the propagating crack. Cavities this small could not be observed by the techniques

described in reference (35). However, because crack velocities and chemical conditions in the MD studies and those in the experiments described in references (17,27) were so different, one might question the equivalence of the MD studies and the subcritical crack growth experiments in moist air.

### Chemistry at Crack Tips

The interaction of water with highly stressed bonds at crack tips has been known for some time and is well documented,<sup>38</sup> but the exact form of water at crack tips is not so well known. It has been hypothesized that a very narrow condensation layer forms at crack tips, the width depending on the relative humidity of the atmosphere.<sup>39</sup> Recent studies by AFM<sup>40-42</sup> have not only demonstrated condensation at crack tips in glass, but have characterized some of the properties of the condensate. Célarie *et al.*<sup>43</sup> demonstrated the diffusion of mobile alkali ions from the condensate region at the crack tip onto the surface of the glass surrounding the crack tip. The condensate formed a parabolic-shaped area ahead of the crack at low velocities, fanning out onto the specimen surface on each side of the crack. The fact that precipitation formed on the specimen surface suggested that the water at the crack tip interacted with the glass to form a solution having

a substantial concentration of ions. An ion exchange of mobile alkali ions in the glass for hydronium ions in the condensate is normally expected, producing a liquid with a substantial pH,<sup>44</sup>  $\approx 12$  for soda lime silicate glass.<sup>45</sup> Such a high pH solution is corrosive to glass and will attack the network to form silicate ions in solution and possibly the condensation of a gel or of dense silicate precipitates.

Support for such an attack on the glass network has been obtained by AFM for static cracks with water at the crack tip.<sup>46</sup> By matching fracture surface sections across the arrested crack front, it can be shown that approximately 10 nm of corrosion has occurred leaving a slot behind in the glass, Fig. 5. The width of the slot depends on the time that the specimen is held under load; the increase in width is approximately parabolic with time.<sup>18</sup>

Other glasses are not expected to have a basic condensate at the crack tip; for these glasses, the rate of corrosion will differ greatly from that of soda lime silicate glass. As can be seen for silica glass, which was held for 80 days under a load of  $K_{\text{appl}} = 0.254 \text{ MPa m}^{1/2}$ , no corrosion notch develops during the hold time in the open portion of the crack, Fig. 6. The reason for the absence of corrosion is that the pH of the condensate at the crack tip is slightly acidic,  $\text{pH} \approx 5$ ,<sup>45</sup> which is not corrosive to silica glass. The dark gray area in Fig. 6, in front of the arrested crack at “a”, is due to a swelling of the glass attributed to water diffusion into the glass at the

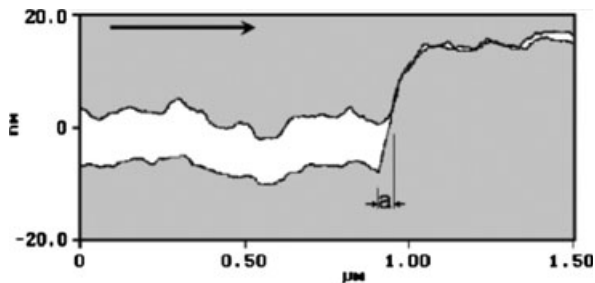


Fig. 5. Matched fracture surface sections across an arrested crack front in soda lime silicate glass. The section across the arrest front is selected by choosing identical marks on the upper and lower surfaces for the section line. The upper and lower fracture surfaces give very good matches in both parts of the fracture surface, that is, before and after crack arrest. The zone marked “a” represents a transition from the open to the closed portion of the crack. The surfaces do not match over this region. The arrow shows the direction of crack growth. Taken from reference (46).

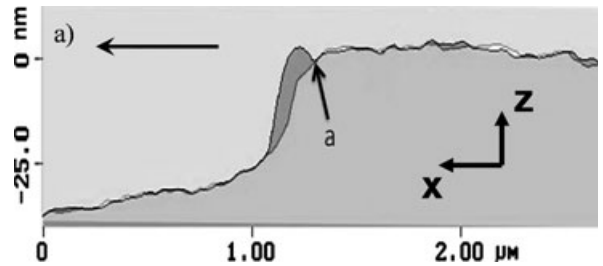


Fig. 6. Matched profiles from an arrested crack in silica glass. The crack arrest point was at point “a.” The surfaces match both before and after the point of crack arrest, indicating no corrosion during the hold time in the fractured part of the specimen. The overlap, dark gray area has been attributed to swelling as a consequence of water diffusion into the glass in front of the crack tip.<sup>19</sup>

crack tip.<sup>20,47</sup> This observation supports the relevance of water penetration at crack tip in silica glass. Further discussions of water penetration into silica glass are given below.

Similar to the compressive stresses that develop at a crack tip with ion exchange in soda lime silicate glass,<sup>18</sup> water penetration at the crack tip of silica glass was shown to induce compressive stresses and to partially shield the crack tip as modeled in reference (47). Such shielding can increase the strength of silica glass,<sup>48</sup> in the same way that shielding increases the strength of transformation toughened  $\text{ZrO}_2$ . The shielding can also change both the slope and position of the  $v$ - $K_I$  curve for silica glass and thus lead to a potentially more crack growth-resistant glass.<sup>20</sup> These effects on silica glass still remain to be explored experimentally.

## Water Condensation

In addition to studying the effect of condensate on the glass at the crack tip, the AFM has been used to characterize the Laplace pressure of the condensate within the crack tip opening.<sup>49</sup> This pressure affects the chemical activity of the water in the condensate, and hence the rate of crack growth for a given applied stress intensity factor. The Laplace pressure also affects the crack tip stress intensity factor. Because of its high negative value the Laplace pressure supplies an extra closing force to crack tip that must be included as part of the driving force for fracture.

To determine the Laplace pressure, two measurements are required: the length of the condensate at the

crack tip and the critical applied stress intensity factor for crack closure. Because the condensate only fills the crack tip to about 100 nm, a high-resolution instrument such as an AFM has to be used to determine the condensate length accurately. This measurement is achieved using the so called tapping mode of measurement. When the probe tip comes in contact with the condensate, a sharp change in retardation is observed and the condensate length can be measured very accurately, Fig. 7. Measured in this way, a Laplace pressure of  $-36 \pm 5$  MPa was determined for a crack tip in silica glass at 40% relative humidity. Also, from the closing forces, an adhesive energy,  $G_o = 180 \pm 20$  mJ/m<sup>2</sup> was obtained, which is reasonably close to the energy required to create two water surfaces, 144 mJ/m<sup>2</sup>.

This technique allows important information to be obtained on the nature of the crack tip condensate, which constitutes the local environment for stress corrosion crack propagation in a moist atmosphere. In silica glass, the condensate composition was shown to be very close to pure water and to be in stationary equilibrium with the moist atmosphere.<sup>42</sup> By contrast, the crack tip condensate size in soda lime silicate glass can evolve in time due to alkali ion diffusion and exchange with hydronium ions at the crack tip.<sup>43</sup>

The coupled modeling of crack tip shielding, induced by water penetration into glass and the evolutions of the local crack tip environment, can be very useful to predict the shape of the  $v$ - $K$  curves in the stress corrosion cracking of silicate glasses as a function of their composition and external environmental.<sup>49</sup>

### Water Penetration at Crack Tips During Crack Growth

The first authors to demonstrate that water penetrated into material surrounding a moving crack in silica glass were Tomozawa *et al.*,<sup>50</sup> who argued that water penetrates because of the dilatation of the silica glass due to the high tensile stresses at the head of the crack tip. As the crack propagates through the water-penetrated glass, the water is left behind on the fracture surface. This water could be detected using the technique of nuclear reaction analysis,<sup>50</sup> which measures the concentration of hydrogen atoms within the glass. The details of the experimental technique are given in reference (50). The resolution of the technique was sufficient to show that the concentration of hydrogen in the water-penetrated surface exceeded that of the oil/etched specimen (cf. caption in Fig. 8) for which adsorbed water was only at the surface.

To obtain a theoretical estimate of the experimental curve in Fig. 8a, the rate of diffusion of water into the tip of a crack from the crack opening has to be calculated. This was performed recently by Wiederhorn *et al.*<sup>47</sup> The diffusion equation for water into glass was solved in cylindrical coordinates and included the effect of the mechanical swelling stresses on the diffusivity. A data curve was estimated from the theoretical penetration curve (the curve calculated in reference 47), and the instrument curve given in the paper by Tomozawa *et al.* (the curve obtained from the oil/etched specimen, Fig. 8). The predicted experimental curve from

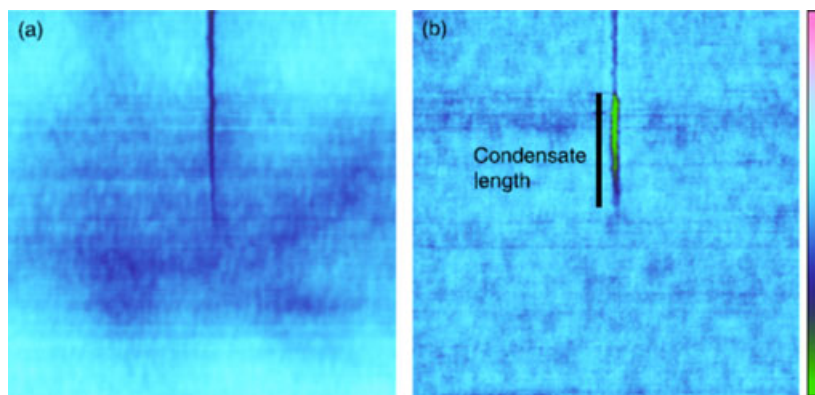


Fig. 7. (a) Typical atomic force microscopy (AFM) height image of a crack tip. Note the depression in the vicinity of the crack tip. (b) Typical AFM phase image of a crack tip. The zone of the phase shift at the front of the crack marks the region of water condensation. The size of the image is 400 nm<sup>2</sup>. The scale to the right of the images is 5 nm for the height image and 5° for the phase image. Taken from reference (49).

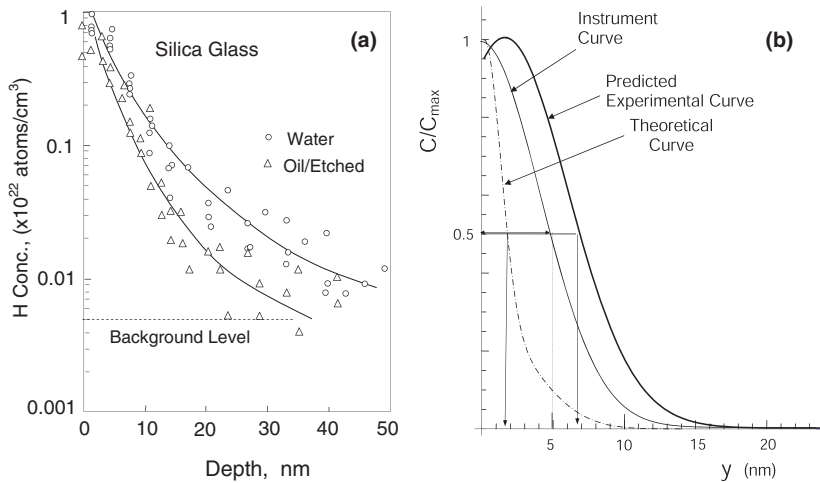


Fig. 8. Hydrogen depth concentration at fresh fracture surfaces. (a) From reference (50). The hydrogen concentration from the specimens that were fractured in water lies significantly to the right of the oil/etched specimen, that is, specimens fractured in oil, or in water then etched in a solution containing HF. The H concentration of the oil/etched specimen is primarily from water adsorbed on the specimen fracture surface. (b) From reference (47). Water Profile (Predicted Experimental Curve) resulting from the convolution of the Theoretical Diffusion Profile for a crack rate of  $v = 10^{-7}$  m/s (dash-dotted curve) with the Gaussian Instrument Curve.

reference (47) was very similar to that measured by Tomozawa *et al.*<sup>50</sup> The half-width at  $0.5 C_{\max}$  for the experimental curve in Tomozawa *et al.* is about 4.5 nm, whereas in Fig. 8b, the half-width of the predicted experimental curve is about 6.6 nm at the same concentration. Although this is a good comparison, one must temper this result with the fact that the instrument curve is very wide relative to the experimental data curve (water curve in Fig. 8a), so that the actual water penetration curve is just a perturbation on the instrument curve. Nevertheless, the fact that perturbation is small suggests a shallow penetration distance. This conclusion is consistent with the theory presented in reference (47).

A second study of water penetration was carried out recently by Lechenault *et al.*,<sup>51</sup> using neutron reflection to study the penetration of deuterium oxide into silica glass. The experimental crack growth technique was similar to that used by Tomozawa *et al.*,<sup>50</sup> but the findings were somewhat different. The penetration depth of the deuterium oxide at half-height was about 6.2 nm at a crack velocity of  $4 \times 10^{-6}$  m/s and 6.7 nm at  $1 \times 10^{-8}$  m/s. These values are slightly higher than those measured by Tomozawa *et al.*<sup>50</sup> Also, Lechenault *et al.* observed an initial plateau in their distribution before an exponential decrease in concentration, in comparison with the monotonic decrease observed by

Tomozawa *et al.* The initial plateau is, however, consistent with the theory presented in reference (47).

Despite these differences, the data indicating penetration of the crack tip in silica by water is suggestive, and, furthermore, is supported both by theoretical calculations using the latest diffusion data for water in silica glass and by the postmortem AFM investigations of fracture surfaces illustrated in Fig. 6. This process of water penetration at crack tips required examination of the fracture surfaces; *in situ* observation of the crack tip by AFM could not have revealed any effect at current levels of magnification.

## Summary

A review is presented with the latest data on the structure of crack tips in glass at the near nanometer level. Measurement techniques are primarily by the atomic force microscopy. We start off with a discussion of surface displacements in the vicinity of a crack ending on a free surface.<sup>24</sup> Measured by AFM, the displacements are elastic at distances greater than 10 nm from the crack surface, indicating that the nonlinear zone at the crack tip is less than 10 nm. As indicated by an elastic-plastic solution of the crack tip,<sup>28,29</sup> the zone size for silica glass is expected to be substantially

less than this. Distances of from 1 nm to 2 nm are suggested by the analysis. A similar result was obtained for an elastic crack with a molecular structure around the crack tip. Therefore, considerable improvement in measurement technique will be needed for *in situ* detection of the nonlinear zone using surface displacement measurements. Examination of fracture surfaces using high-resolution techniques other than AFM has the capacity to reveal details about the crack tip structure at a resolution of better than 10 nm. Thus, water penetration into crack tips of 5–8 nm has been demonstrated by nuclear reaction analysis<sup>50</sup> and neutron reflection.<sup>51</sup> AFM measurements on fracture surfaces reveal details of the crack tip structure at the nm level for crack tip corrosion<sup>46</sup> and for water penetration into crack tips of glass.<sup>20,47</sup> *In situ* AFM phase imaging measurements also reveal important information on the local environment at crack tips.<sup>40,42,49</sup> As the resolution of the measurement techniques improves, a similar improvement on details of the nonlinear zones at crack tips in glass is expected. Thus, the details of the crack tip structure that eluded Griffith are expected to become available at higher resolution for future investigators of crack tip structure.

## References

1. A. A. Griffith, "The Phenomena of Rupture and Flow in Solids," *Philos. Trans. Roy. Soc. London, A*, 221 163–198 (1921).
2. G. C. Sih, P. C. Paris, and G. R. Irwin, "On Cracks in Rectilinearly Anisotropic Bodies," *Int. J. Fract. Mech.*, 1 [3] 189–203 (1965).
3. D. M. Marsh, "Plastic Flow and Fracture of Glass," *Proc. Roy. Soc. (London)*, 282A [1388] 33–43 (1964).
4. B. J. Hockey and B. R. Lawn, "Electron Microscopy of Microcracking About Indentations in Aluminum Oxide and Silicon Carbide," *J. Mater. Sci.*, 10 1275–1284 (1975).
5. B. R. Lawn, B. J. Hockey, and S. M. Wiederhorn, "Atomically Sharp Cracks in Brittle Solids: An Electron Microscopy Study," *J. Mater. Sci.*, 15 1207–1223 (1980).
6. W. B. Hillig, "Plastic Behavior and Fracture in Glass," *Microplasticity*, eds., C. J. McMahon. Interscience, New York, p. 383, 1968.
7. A. Kelly, W. R. Tyson, and A. H. Cottrell, "Ductile and Brittle Crystals," *Philos. Mag.*, 15 576 (1967).
8. J. R. Rice and R. Thomson, "Ductile Versus Brittle Behavior of Crystals," *Philos. Mag.*, 29 [1] 73–97 (1974).
9. S. M. Wiederhorn, B. J. Hockey, and D. E. Roberts, "Effect of Temperature on the Fracture of Sapphire," *Phil. Mag.*, 28 783–796 (1973).
10. H. Tanaka, Y. Bando, Y. Inomata, and M. Mitomo, "Atomically Sharp Crack in 15R-SiAlON," *J. Am. Ceram. Soc.*, 71 [1] C32–C33 (1988).
11. H. Tanaka and Y. Bando, "Atomic Crack Tips in Silicon-Carbide and Silicon-Crystals," *J. Am. Ceram. Soc.*, 73 [3] 761–763 (1990).
12. D. R. Clarke and K. T. Faber, "Fracture of Ceramics and Glasses," *J. Phys. Chem. Solids*, 48 [11] 1115–1157 (1987).
13. Y. Bando, S. Ito, and M. Tomozawa, "Direct Observation of Crack Tip Geometry of SiO<sub>2</sub> Glass by High-Resolution Electron-Microscopy," *J. Am. Ceram. Soc.*, 67 C36–C37 (1984).
14. S. M. Wiederhorn, "Fracture Surface Energy of Glass," *J. Am. Ceram. Soc.*, 52 [2] 99–105 (1969).
15. P. Eaton and P. West, *Atomic Force Microscopy*, Oxford University Press, New York, 2010.
16. S. M. Wiederhorn, J.-P. Guin, and T. Fett, "The use of Atomic Force Microscopy to Study Crack Tips in Glass," *Met. Mater. Trans.*, 42A 2011–2267 (2011).
17. F. Célerié, *et al.*, "Glass Breaks Like Metals, but at the Nanometer Scale," *Phys. Rev. Lett.*, 90 [7] 075504 (2003).
18. T. Fett, J. P. Guin, and S. M. Wiederhorn, "Interpretation of Effects at the Static Fatigue Limit of Soda-Lime-Silicate Glass," *Eng. Fract. Mech.*, 72 [18] 2774–2791 (2005).
19. S. M. Wiederhorn, T. Fett, G. Rizzi, S. Fünfschilling, M. J. Hoffmann, and J.-P. Guin, "Effect of Water Penetration on the Strength and Toughness of Silica Glass," *J. Am. Ceram. Soc.*, 94 [6] S196–S203 (2011).
20. S. M. Wiederhorn, T. Fett, G. Rizzi, M. Hoffmann, and J.-P. Guin, "Water Penetration – Its Effect on the Strength and Toughness of Silica Glass," *Met. Mater. Trans. A*, 44 [3] 1164–1174 (2013).
21. C. Janssen, "Specimen for Fracture Mechanics Studies on Glass," In: Proceedings of the Xth International Congress on Glass. Kyoto, Japan, 1974. p. 23.
22. T. A. Michalske and E. R. Fuller Jr, "Closure and Repropagation of Healed Cracks in Silicate Glass," *J. Am. Ceram. Soc.*, 68 586–590 (1985).
23. T. Fett, G. Rizzi, J. P. Guin, J. M. López-Cepero, and S. M. Wiederhorn, "A Fracture Mechanics Analysis of the Double Cleavage Drilled Compression Test Specimen," *Eng. Fract. Mech.*, 76 921–934 (2009).
24. K. Han, M. Ciccotti, and S. Roux, "Measuring Nanoscale Stress Intensity Factors With an Atomic Force Microscope," *EPL*, 89 66003 (2010).
25. T. Fett, *et al.*, "Finite Element Analysis of a Crack tip in Silicate Glass: No Evidence for a Plastic Zone," *Phys. Rev. B*, 77 174110 (2008).
26. S. Roux and F. Hild, "Stress Intensity Factor Measurements From Digital Image Correlations: Post-Processing and Integrated Approaches," *Int. J. Fract.*, 140 [1–4] 141–157 (2006).
27. S. Prades, D. Bonamy, D. Dalmas, E. Bouchaud, and C. Guillot, "Nano-Ductile Crack Propagation in Glasses Under Stress Corrosion: Spatiotemporal Evolution of Damage in the Vicinity of the Crack tip," *Int. J. Solids Struct.*, 42 [2] 637–645 (2005).
28. D. S. Dugdale, "Yielding of Steel Sheets Containing Slits," *J. Mech. Phys. Solids*, 8 100–104 (1960).
29. G. I. Barenblatt, "The Mathematical Theory of Equilibrium Cracks in Brittle Fracture," *Advances in Applied Mechanics*, Vol. 7, eds., H. L. Dryden and T. von Harman. Academic Press, New York, 55–129, 1962.
30. C. R. Kurkjian, P. K. Gupta, R. K. Brow, and N. Lower, "The Intrinsic Strength and Fatigue of Oxide Glasses," *J. Non-Cryst. Solids*, 316 114–124 (2003).
31. B. R. Lawn, K. Jakus, and A. C. Gonzalez, "Sharp vs. Blunt Crack Hypotheses in the Strength of Glass: A Critical Study Using Indentation Flaws," *J. Am. Ceram. Soc.*, 68 [1] 25–34 (1985).
32. M. Creager and P. C. Paris, "Elastic Field Equations for Blunt Cracks With Reference to Stress Corrosion Cracking," *Int. J. Fract.*, 3 247–252 (1967).
33. W. Weibull, "A Statistical Theory of the Strength of Materials," *Ingenjörsvetenskaps Akad. Handl.*, 151 1–45 (1939).
34. T. L. Anderson, *Fracture Mechanics*, CRC Press, Boca Raton, FL, 1995.
35. J.-P. Guin and S. M. Wiederhorn, "Fracture of Silicate Glasses: Ductile or Brittle?" *Phys. Rev. Lett.*, 92 [21] 215502 (2004).
36. J. M. López-Cepero, S. M. Wiederhorn, T. Fett, and J.-P. Guin, "Do Plastic Zones Form at Crack Tips in Silicate Glasses?" *Int. J. Mater. Res.*, 98 [12] 1170–1176 (2007).
37. C. L. Rountree, R. K. Kalia, E. Lidorikis, A. Nakano, L. V. van Brutzel, and P. Vashishta, "Atomistic Aspects of Crack Propagation in Brittle Materials: Multimillion Atom Molecular Dynamics Simulations," *Annu. Rev. Mater. Res.*, 32 377–400 (2002).
38. S. W. Freiman, S. M. Wiederhorn, and J. J. Mecholsky, "Environmentally Enhanced Fracture of Glass: A Historical Perspective," *J. Am. Ceram. Soc.*, 92 [7] 1371–1382 (2009).
39. S. M. Wiederhorn, "Influence of Water Vapor on Crack Propagation in Soda-Lime Glass," *J. Am. Ceram. Soc.*, 50 [8] 407–414 (1967).
40. L. Wondraczek, A. Dittmar, C. Oelgardt, F. Celarie, M. Ciccotti, and C. Marliere, "Real-Time Observation of a non-Equilibrium Liquid

- Condensate Confined at Tensile Crack Tips in Oxide Glasses,” *J. Am. Ceram. Soc.*, 89 [2] 746–749 (2006).
41. M. Ciccotti, M. George, V. Ranieri, L. Wondraczek, and C. Marlière, “Dynamic Condensation of Water at Crack Tips in Fused Silica Glass,” *J. Non-Cryst. Solids*, 354 564–568 (2008).
  42. A. Grimaldi, M. George, G. Pallares, C. Marlière, and M. Ciccotti, “The Crack tip: A Nanolab for Studying Confined Liquids,” *Phys. Rev. Lett.*, 100 165505 (2008).
  43. F. Celarie, M. Ciccotti, and C. Marlière, “Stress-Enhanced ion Diffusion at the Vicinity of a Crack tip as Evidenced by Atomic Force Microscopy in Silicate Glasses,” *J. Non-Cryst. Solids*, 353 [1] 51–68 (2007).
  44. R. H. Doremus, *Glass Science*, 2nd edition, John Wiley & Sons Inc., New York, 1994.
  45. S. M. Wiederhorn, “A Chemical Interpretation of Static Fatigue,” *J. Am. Ceram. Soc.*, 55 [2] 81–85 (1972).
  46. J.-P. Guin, S. M. Wiederhorn, and T. Fett, “Crack-Tip Structure in Soda-Lime-Silicate Glass,” *J. Am. Ceram. Soc.*, 88 [3] 652–659 (2005).
  47. S. M. Wiederhorn, T. Fett, G. Rizzi, M. J. Hoffmann, and J. P. Guin, “The Effect of Water Penetration on Crack Growth in Silica Glass,” *Eng. Fract. Mech.*, 100 3–16 (2013).
  48. T. Fett, G. Rizzi, M. J. Hoffmann, S. Wagner, and S. M. Wiederhorn, “Effect of Water on the Inert Strength of Silica Glass: Role of Water Penetration,” *J. Am. Ceram. Soc.*, 95 [12] 3847–3853 (2012).
  49. G. Pallares, A. Grimaldi, M. George, L. Ponson, and M. Ciccotti, “Quantitative Analysis of Crack Closure Driven By Laplace Pressure in Silica Glass,” *J. Am. Ceram. Soc.*, 94 [8] 2613–2618 (2011).
  50. M. Tomozawa, W.-T. Han, and W. A. Lanford, “Water Entry Into Silica Glass During Slow Crack Growth,” *J. Am. Ceram. Soc.*, 74 [10] 2573–2576 (1991).
  51. F. Lechenault, D. L. Rountree, F. Cousin, J. -P Bouchaud, L. Ponson, and E. Bouchaud, “Evidence of Deep Water Penetration in Silica During Stress Corrosion Fracture,” *Phys. Rev. Lett.*, 106 165504 (2011).